EUROPEAN ORGANIZATION FOR NUCLEAR RESEARCH

CERN/ISRC/74-45
4 October 1974

ADDENDUM TO THE PROPOSAL ISRC 74/38

SEARCH FOR ELECTRONS AND MUONS DIRECTLY PRODUCED IN THE FORWARD DIRECTION: A HUNT FOR CHARMED PARTICLES

L Baum
M Block
J Crawford
A Derevshchikov
R Glauber
I. Golutvin
H Hilscher
J Irion
A Kernan
V Kukhtin
J Layter
W Marsh
F Muller
P McIntyre
B Naroska
M Nussbaum
A Orkin-Lecourtois
C Rubbia
D Schinzel
B Shen
A Staude
G Tarnopolsky
V Telegdi
R Voss

CERN, Geneva, Switzerland

Department of Physics, Harvard University,
Cambridge, Mass , USA

Sektion Physik der Universität, Munich, Germany

Northwestern University, Evanston, Ill , USA

University of California at Riverside,
Riverside, Calif , USA

1 INTRODUCTION

The present document describes the progress since the time of submission of proposal ISRC/74-38, a Search for Charmed Particles at the ISR [1] It also gives a detailed time-table for the initial phases of the experiment, under the assumption that the final approval will be given at the next ISRC meeting

The experiment has been described in the document ISRC/74-38 [1] which remains substantially valid Briefly, it consists in identifying production and decay of "charmed" particles by the observation of muons and/or electrons originating from the interaction point, eventually in association with an anomalously copious strange-particle yield The R604 spectrometer can be converted with relatively trivial additions into a muon and strange-particle detector Electrons, instead, need a novel detecting apparatus Finally, for optimum conditions, the vacuum chamber must be modified in order to reduce $\pi \rightarrow \mu$ decay background before the muon filter and γ-ray conversion before the electron telescope

We have made considerable progress in the preparation of the electron telescope:

1) We have found a much better suited analysing magnet We have redesigned the electron telescope around this new magnet (see Section 2) and we have been able to achieve an acceptance approximately 20 times larger than the one of the previous design[1]

2) We have carried out extensive tests of a gas Čerenkov counter in an electron and pion beam at the CERN PS On the basis of these measurements we have determined the optimal radiator length and we have achieved a satisfactory rejection figure for pions (see Section 3) We are confident that these figures can be further improved in the final detector

3) Proportional chambers (drift-type) are ready All the requisite electronic modules including the CAMAC interface, are at present available to us

4) We intend to use 20 of the 84 lead-glass blocks of the recently completed Steffen-Steinberger experiment on the Σ^0 lifetime They will ensure simple coverage of the increased solid angle

The electron detector is at present defined in all its details Since most of the hardware is already in our hands, we are confident that we can proceed as follows:

i) assembly in about one month,
ii) testing in the PS beam during the first two weeks of November, and
iii) installation in I6 before the beginning of ISR-period 9

The enlarged acceptance of the electron telescope requires new rate and background evaluations We have written a very detailed Monte Carlo calculation which traces events through specified production and decay mechanisms Although the theoretical understanding of the production mechanism and of decay branching ratios is not on a firm footing, calculations have been a very powerful tool for our experimental design (see Section 4)

The ISR vacuum group has indicated that even assuming the firmest instruction from the ISRC, the new vacuum chamber cannot be fabricated and installed before the end of February 1975, which would then delay the beginning of the experiment to about March 1975 We believe that any delay in the beginning of our experiment would be inappropriate because of the frenetic and well supported competition coming from FNAL Consequently we propose to subdivide our experiment into two phases with the changeover of the vacuum chamber between Phases I and II The experimental layout of Phase I is shown in Fig 1 In this phase, the muon filter is located behind the magnetic spectrometer, and the electron detector can be placed at any angle between 30° and 90° The $\pi \to \mu$ decay probability (before the filter) is $\sim$ 0 02 for a 5 GeV/c pion and the electrons have to traverse of the order of 0 02 radiation lengths For comparison, the corresponding value for the Phase II set-up (Fig 2), where the iron filter is located in front of the spectrometer and the window for the electrons is only 0 006 radiation lengths, is 0 002 for $\pi \to \mu$ decay probability

Very roughly, the muon-electron coincidence background is larger in Phase I than in Phase II by a factor

$$\frac{0\ 02}{0\ 002} \times \frac{(0\ 02 + 0\ 00625)}{(0\ 006 + 0\ 0065)} = 20$$

[The factor 0 00625 has been added in order to take into account the internal (Dalitz) conversion probability]

The detection efficiency for "charmed" muon-electron coincidences is roughly the same in the two phases, the losses of acceptance of the electron telescope of Phase I being almost exactly compensated by the increased acceptance of the muon telescope However, the invariant mass resolution and the acceptance for di-muons is considerably better during Phase I, since the multiple scattering in the muon filter does not affect the precision of the measurements and the whole aperture of the spectrometer becomes useful for muon detection

Finally the angle of the electron telescope can be varied during Phase I, whereas it is fixed during Phase II

In summary, the physics objectives of Phase I are as follows:

1) Installation, tuning and testing of all the components of the experiment

2) Observation of the inclusive electron yield for angles $\geq 30^\circ$ and a first attempt to search for lepton-lepton coincidences

3) A sensitive search for the vector meson ϕ_C made of a $(p'\overline{p'})$ bound state in the "charmed" analogue to the ordinary ϕ-meson, which is a $(\lambda\bar{\lambda})$ state[2] This new object, which must exist according to SU(4), is expected to have most of its decay modes suppressed, an enhanced leptonic branching ratio $\Gamma(\phi_C \to \mu^+\mu^-$ or $e^+e^-)/\Gamma_{\phi_C} \approx 1\%$, and a very narrow width, $\Gamma_{\phi_C} \approx 2$ MeV The excellent mass resolution in Phase I (coupled with an adequate background rejection) makes it an ideal instrument for this search

Phase II should take over after two to four ISR periods, depending on the progress of the vacuum chambers We can then proceed to the final search for muon-electron coincidences Note that the study of $\phi_C \to \mu^+\mu^-$ decays can also be pursued during Phase II, simply by changing the iron absorber from the front to the back of the spectrometer

2 DETAILED DESIGN OF THE ELECTRON DETECTOR

The experimental set-up already described in the document CERN/ISRC/74-38 [1] consists of a magnetic spectrometer in arm 1, a spectrometer with calorimeters in arm 2, and the electron arm We have studied in more detail the electron arm, which is the only additional component to the R604 equipment We plan to enlarge the acceptance of this arm, using a larger magnet, larger chambers, and more lead-glass blocks Furthermore, a short Čerenkov counter for separating electrons from pions has been successfully tested

The electron arm is shown in Fig 1 Electrons enter the spectrometer through a 0 13 mm thick circular window of 240 mm diameter A window of such small thickness has already been produced and tested by the ISR vacuum group; tooling exists

Three sets of drift chambers identify the track Each set consists of four planes: two planes with horizontal and two planes with vertical wires The planes are staggered to resolve the left-right ambiguity of the drift chambers A single plane is shown in Fig 3 In addition to the coordinate information, the chambers provide an analogue signal proportional to the ionization loss and thus allow discrimination of small-angle pairs The energy resolution of one gap for a minimum ionizing particle was measured to be 60% FWHM The pulse-height spectrum is shown in Fig 4 The chambers exist and have been tested

The magnet, constructed by the ISR, has an aperture of 40 × 25 cm^2 and a bending power of ∿ 0 5 Tm The power consumption is 80 kW

The Čerenkov counter will fill the available magnet gap and will extend slightly beyond the magnet ends to give a total radiator length of 110 cm Three UV-sensitive phototubes will be used Based on the experimental results which are described in Section 3, pion rejection of 10^3 with an electron detection efficiency of 90% can be achieved by demanding a signal corresponding to more than two photoelectrons Fifteen lead-glass blocks, arranged in a matrix of 5 × 3 blocks at the end of the spectrometer, cover the acceptance These counters, 15 × 15 × 35 cm^3 each, can be made available to us by the Steffen-Steinberger group

We expect a rejection capability against hadrons of about 10^6 and a detection efficiency of ∿ 85% for the whole arm These numbers are the results of the following requirements:

i) the momentum measured by magnetic deflection and the momentum measured by the Pb-glass-counters agree, giving a rejection against hadrons of better than 10^2 [3];

ii) the Č-counter gives a rejection of 10^3 with an electron efficiency of 90%;

iii) the additional Pb-shower-counters, $5x_0$ each, in front of the Pb-glass matrix give a rejection of better than 100 [3,4]

For the identification of background events due to Dalitz pairs and γ conversion in the material before the first chamber we have two criteria:

i) agreement of the energy measured with the lead-glass and the magnet;

ii) pulse-height in the scintillation counters and drift chambers corresponding to a single particle

The remaining background can be measured by inserting additional material in front of the electron telescope and extrapolating to zero thickness[5]

The parameters of the telescope are summarized in Table 1

As outlined in the introduction, we intend to use this telescope already in a first phase of the experiment with the vacuum chamber installed at present in I6 (Fig 5) The telescope can be installed at angles between 30° and 90°. For this angular range the effective wall thickness of the bicone ranges between 0 45 and 0 2 mm

Table 1

Parameters of the electron telescope

1	Vertical acceptance	$\sim$ 0 1 rad
2	Horizontal acceptance	$\sim$ 0 17 rad
3	Solid angle	$\sim$ 0.017 ster
4	Momentum resolution of the magnetic spectrometer	$\sim \pm 1$ 5%
5	Energy resolution of the lead-glass	$\sim$ 5 ÷ 6% (FWHM)
6	Rejection capability against pions	$\sim 10^6$
7	Electron detection efficiency	$\sim$ 85%
8	Total amount of material before the first drift chamber	$\sim$ 0 02 x_0

3 TESTS ON THE GAS ČERENKOV COUNTER

The gas Čerenkov counter is a relatively critical part of the detector, since it must be as short as possible, still retaining a good detection efficiency and an effective rejection against pions In order to test the design concepts, we have performed some measurements at the CERN PS A Čerenkov counter with a 1 m radiator pipe was equipped as shown in Fig 6 with an RCA 31000 M photomultiplier tube This tube, having a bi-alkali cathode on a quartz window, has a spectral response extending from $\sim$ 1800 to $\sim$ 5500 Å, and its high-gain first dynode ("quantacon") allows reliable calibration of the output signal in terms of photo-electrons emitted by the cathode Air at atmospheric pressure was used as a radiator, and there was no extra window at the exit of the parabolic collector

In the first part of the test, a beam of 500 MeV/c electrons was used, and a thin piston was moved in steps to vary the Čerenkov radiator length The result is shown in Fig 7 and is consistent with a straight line through the origin, whose slope is 4.0 photoelectrons/metre.

In the second part, 1 GeV/c muons, which were well below the Čerenkov threshold of $\sim$ 6 GeV/c, were used The output signal was pulse-height analysed, and the detection efficiency for pions (including noise) was derived as a function of the threshold requirement of the device The result is shown in Fig 8, together with the electron detection efficiency calculated from Poisson statistics

It is concluded that a pion rejection of $10^3 : 1$ with $\sim$ 90% detection efficiency for electrons can be achieved with a radiator of 110 cm of length and a threshold requirement of > 2 photoelectrons

We believe that the residual detection efficiency for pions is due to emission of δ-rays and to slight scintillation of air We think we can further reduce these effects by operating the counter in the magnetic field of the spectrometer and by "poisoning" the gas with some small addition of ethylene or of a similar gas Tests are in progress

The final Cerenkov counter is expected to have a somewhat higher light-collection efficiency, since the mirrors used for the test did not have a surface coating of sufficiently good quality for UV light

4 RATES AND BACKGROUNDS

Using a Monte Carlo technique we have calculated the acceptance of this experiment for the decay products of charmed particles We have obtained event rates and backgrounds for the two cases of interest -- diffractive production and inclusive production in the configuration of phase II.

4 1 Diffractive production*)

We begin with the excitation of a diffracted system N^* with invariant mass M and squared momentum transfer t, according to $d\sigma/dM^2dt \propto (1/M^2)\, e^{6t}$ This system then dissociates via the channel

$$N^* \to N' + \bar{\pi}' + (n\pi)$$

into a charmed baryon, a charmed boson, and a multipion system; we assume a mean pion multiplicity of 3 and invariant mass $m_{n\pi}$ = 0 5 GeV/c^2 We assume a flat Dalitz plot in the three-body phase space, obtaining the momenta $\vec{p}_{N'}$ and $p_{\bar{\pi}'}$. The charmed particles now decay leptonically via

$$N' \to Y + \ell^+ + \nu_\ell$$

$$\bar{\pi}' \to K + \ell^- + \bar{\nu}_\ell \ ,$$

where $Y = \Sigma^{\pm 0}$ or Λ, $K = K^+$ or K^0, and $\ell = \mu$ or e We have assumed a (V - A) matrix element for these decays and obtain $\vec{p}_Y$, $\vec{p}_K$, $\vec{p}_{\ell^+}$, $\vec{p}_{\ell^-}$.

---

*) We adopt the model of diffractive production of charmed particles given in the internal R604 report of M M Block (see Appendix)

Assuming $\ell = \mu$, we project $\vec{p}_{\mu^\pm}$ through the steel filter, accounting for multiple scattering and a magnetic field in the steel, and obtain the acceptance of the spectrometer Assuming $\ell = e$, we project $\vec{p}_{e^\pm}$ into the electron arm, and calculate the acceptance as a function of energy cut-off We also look for K^+, $\Lambda \to p + \pi^-$, $K_S^0 \to \pi^+ + \pi^-$ in the central (< 0 050 rad) region of the spectrometer All event topologies are required to yield an observable (> 0 010 rad) proton in arm 2

The resulting angular distributions and spectra of acceptance events are shown in Fig 9 for electrons and Fig 10 for muons. The acceptances for the various event topologies of interest are presented in Table 2. From these acceptances A_i we calculate event rates as follows:

$$\text{Rate} = \mathscr{L}\sigma_C \prod_i (BR_i A_i) \ , \quad i = 2 \text{ or } 3$$

where $\mathscr{L} = 4 \times 10^{30}$ cm^{-2} sec^{-1}, $\sigma_C = 0\ 5$ mb, $BR_e = BR_\mu = \frac{1}{2}BR_\ell$, $BR_{K^0} = \frac{1}{2} \times 0\ 37$, $BR_{K^+} = \frac{1}{2}$, $BR_\Lambda = \frac{1}{2} \times 0\ 64$, $A_{p_2} = 0\ 37$. The expected rates are presented in Table 3 for $BR_\ell = 0.1$

The dependence of the lepton acceptances on various experimental parameters -- magnetic field in the steel, masses of N′ and π′, and $\sqrt{s}$ -- are shown in Figs 11 and 12. Additionally, the acceptances are insensitive to the mass $m_{n\pi}$ and the (V - A) mixture governing the charm decays.

We found that the primary sources of background are $\pi^\pm \to \mu^\pm + \nu_\mu$ into the muon spectrometer and $\pi^0 \to \gamma + e^+ + e^-$ Dalitz decays into the electron arm. We used the same model for diffractive production of N^*, and looked at the channel

$$N^* \to p + \pi + (n\pi)$$

The analysis then proceeded as before, tracing the π decays into the acceptance of the experiment The $\pi^\pm$ were required to decay before 1 absorption length in the steel if accepted The $e^\pm$ from Dalitz decay were required to have an opening angle of > 0 040 rad or one member with < 5 MeV to be accepted as a single electron. The resulting acceptances are presented in Table 4, along with event rates calculated on the following basis:

$$\text{Rate} = \mathscr{L}\sigma_D A_\ell^\pi A_{p_2} \ ,$$

where $\sigma_D = 5$ mb is the diffractive cross-section for each charge of pion. Note that we have an effective signal-to-background ratio of ∿ 15:1 for single muons, 50:1 for single electrons.

Another source of background, pion punch-through, should play a role that is small with respect to π decay before the steel, since the requirement of a single minimum ionizing particle in counters segmented in the steel reduces the punch-through probability to $e^{-\ell/\lambda_0} \simeq 5 \times 10^{-5}$ This is compensated by less than a factor of 10 in the decay path, so it is negligible compared to decays before the steel

Table 2

Acceptance for charm decay products
(diffractive charm production)

Event topology	Acceptance $\times 10^5$		
Cut-off $E_e >$	2	3	4 GeV
μ^+	3800		
μ^-	4000		
e^+	540	400	270
e^-	470	320	210
$e^+\mu^-$	20	12	4
$e^-\mu^+$	18	7	3
$\mu^+\mu^-$	120		
$\mu^+\Lambda$	10		
μ^-K^0	20		
μ^-K^+	300		
$e^+\Lambda$	7	3.5	2
e^-K^0	1 5	1.5	0
e^-K^+	45	25	10

Acceptance for diffracted proton p_2	
Minimum vertical p_2 angle	Acceptance
0.005	0.67
0.010	0.37
0 015	0.18

Table 3

Rates for charm decay products
(diffractive charm production)

Event topology	Events per day		
Cut-off E_e >	2	3	4 GeV
e^+p_2	17000	13000	8500
e^-p_2	15000	10000	6700
$e^+\mu^-p_2$	30	18	6
$e^-\mu^+p_2$	30	12	5
$e^+\Lambda p_2$	70	30	20
$e^-K^+p_2$	700	400	150
$\mu^-\Lambda p_2$	100		
$\mu^-K^+p_2$	4500		
$\mu^+\mu^-p_2$	200		

Input assumptions:

1) no magnetic field in steel μ filter
2) electron acceptance at $\theta = (20 \pm 5)^\circ$, $\phi = \pm 1.5^\circ$
3) minimum p_2 angle = 0.010 rad
4) luminosity = 4×10^{30} cm^{-2} sec^{-1}
5) total charm production = 0.5 mb
6) leptonic branching ratio = 0.1
7) branching ratio for K^0 = 0.5×0.35
   K^+ = 0.5
   Λ = 0.5×0.64

Table 4

Backgrounds from diffractive production

Background source	Acceptance × 10^5		
Cut-off E_e >	2	3	4 GeV
$\pi^{\pm} \to \mu^{\pm} + \nu$	3		
$\pi^0 \to \gamma + e^+ + e^-$	0.10	0 05	0.02
	Events per day		
Cut-off E_e >	2	3	4 GeV
$\mu^+\mu^- p_2$	0 6		
$e\mu p_2$	0 010	0 005	0 002
ep_2	750	600	400

Comparing tables 3 and 4, we see that with the assumptions made about diffractive production (σ = 0 5 mb) and leptonic branching ratio (BR = 10%), the signal (S) to background (B) ratios are 60 : 0 01 = 6000 for the $\mu e p_2$ signal and 200 : 0 6 = 330 for the $\mu\mu p_2$ signal This means that, if the product $\sigma(BR)^2$ is actually 100 times smaller, i e equal to 0 05 μb, we still get 0 6 $ue p_2$ events per day, with S/B = 60 and 2 $\mu\mu p_2$ events per day, with S/B = 3 3 From the standpoint of signal only, the situation is even better for the lepton -- strange particle final states, where the signal goes linearly with the leptonic branching ratio

4 2 Inclusive charm production

As mentioned in the original proposal and discussed in more detail in the Appendix, charm production can occur through pair production, analogously to $p\bar{p}$ production We have calculated our yield for such an inclusive process, using the measured (x, p_T) distribution for antiprotons as our production model for inclusive charmed particle-pair-production The charm pair production cross-section was normalized such as to account for the lepton production at 90° observed at NAL and ISR

We find signal rates μe = 8 events/day and μμ = 15 events/day (BR_ℓ = 0 1 and N′ mass = 3 GeV), whereas predicted background from inclusive π production is about 15 per day for μe and 1400 per day for μμ (refer to Table II of ISRC 74/38)

The rates are about 10 times smaller than for diffractive production (due to the fact that inclusive pair production occurs preferentially in the central region), whereas backgrounds are more than 1000 times greater than backgrounds in the diffractive process Clearly, and as expected, our experiment is better suited for this latter process; however μ_e signals from charm inclusive production could be observed, if $BR_\ell > 0\ 2$ Also, the numbers 8 (signal, in the 2 unlike charge channels only) and 15 (background, about equally distributed in the 4 charge channels) allow with a few days of running a meaningful comparison of the unlike and like charge channels

4 3 Hidden charms

As outlined in Section 1, mesons built from a pair of $p', \overline{p'}$ quarks are expected to decay in K^+K^- and, with a branching ratio $\gtrsim$ 1% in lepton -pairs The K^+K^- decay mode is well accessible in the spectrometer without Fe-absorber in front (phase I), as discussed in the initial proposal, ISRC 74-38 (see Section 5 about vector mesons)

The leptonic mode $\mu^+\mu^-$ can be detected both in phase I (with more background, but high mass resolution) and in phase II Typical values for the acceptance of our apparatus in phase I are as given in ISRC 74-38; in phase II, the acceptance is limited for each μ by the solid angle covered by the Fe-absorber; in the forward production region, acceptances of more than 1% are obtained for "hidden charm" mesons of masses 1, 1 5, 2 GeV/c with momenta greater than 8, 10, 12 GeV/c respectively

5 CONCLUSION

The design of the apparatus was aimed at the detection of forward produced charmed particles More specifically, rates -- backgrounds were calculated in the case of associated charm production in a diffractive process, and the parameters of the experimental set-up were optimized accordingly The result is that, in this process, we are sensitive (at the level of about 1 event per day and good signal to background ratio) to a value of the product $\sigma_C (BR)^2 = 0\ 05\ \mu b$

REFERENCES

1) L Baum et al., CERN/ISRC/74-38

2) See, for instance, "Search for Charm", M.K. Gaillard et al , FERMILAB-PUB-74/86-THY

3) B J Blumenfeld et al , CERN/ISRC/73-13

4) B J Blumenfeld et al., Nuclear Instrum Methods 97, 427 (1971)

5) J A Appel, NAL-PUB-74/71-EXP, 7100 070

Figure captions

Fig. 1 : Schematic layout, phase I.

Fig. 2 : Muon filter and electron telescope, phase II.

Fig. 3 : Drift chamber.

Fig. 4 : Pulse-height distribution in drift chamber.

Fig. 5 : Electron telescope, phase I

Fig. 6 : Test Čerenkov counter.

Fig. 7 : Yield of Čerenkov.

Fig. 8 : Efficiency of Čerenkov

Fig. 9a : Angular distribution of charm-produced electrons, showing telescope acceptance.

Fig. 9b : Spectrum of charm-produced electrons in telescope acceptance.

Fig. 10a : Spectrum of charm-produced μ^+ after steel.

Fig. 10b : Spectrum of charm-produced μ^- after steel.

Fig. 11 : Effect on $\mu^\pm$ acceptance of a field B in steel absorber.

Fig. 12a : Effect on $\mu^\pm$ acceptance of masses $M_{N'}$, $M_{\pi'}$.

Fig. 12b : Effect on $\mu^\pm$ acceptance of proton energy $\sqrt{s}/2$.

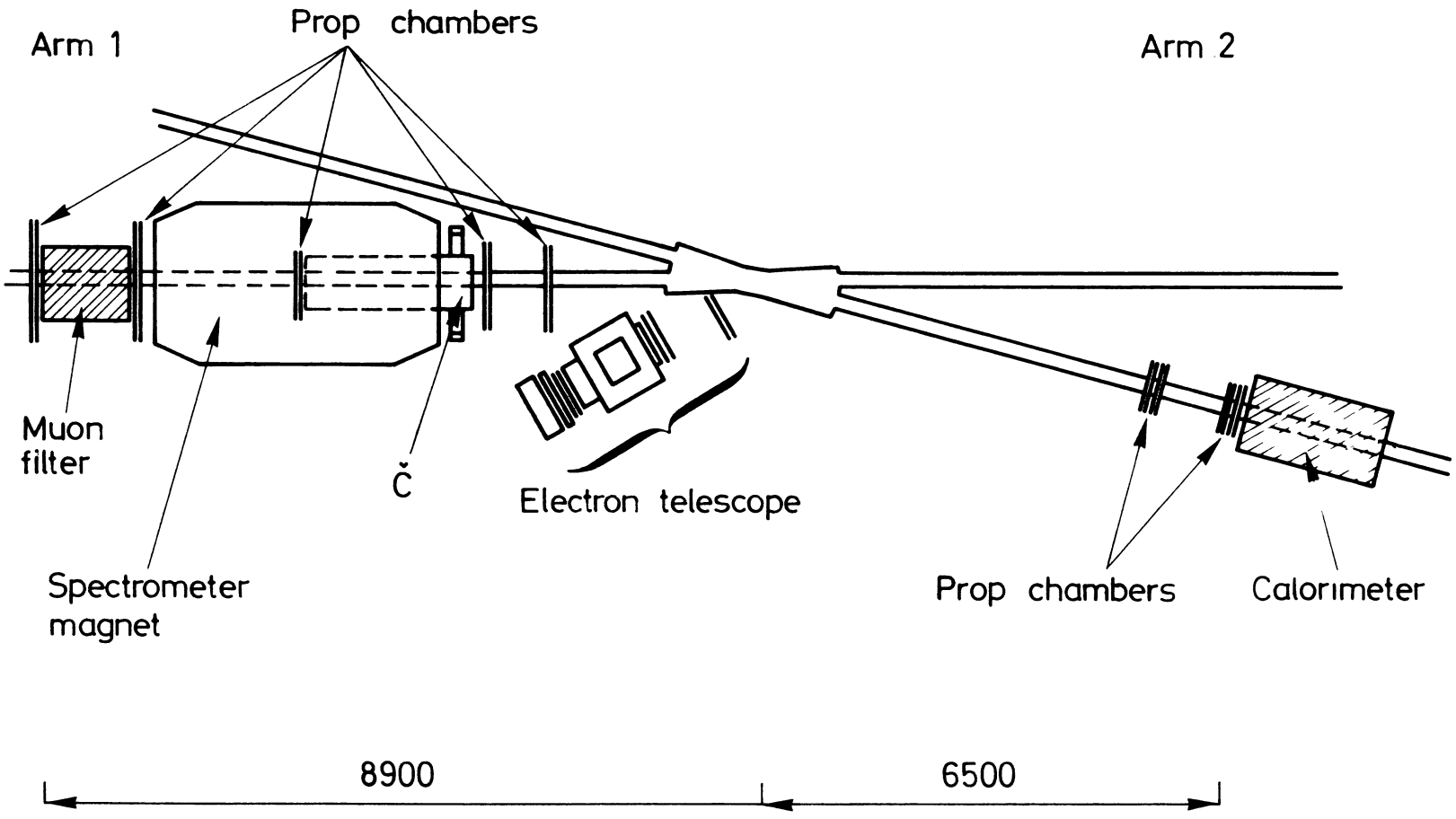
Arm 1
Prop chambers
Arm 2
Muon filter
Č
Electron telescope
Spectrometer magnet
Prop chambers
Calorimeter
8900
6500

FIG. 1

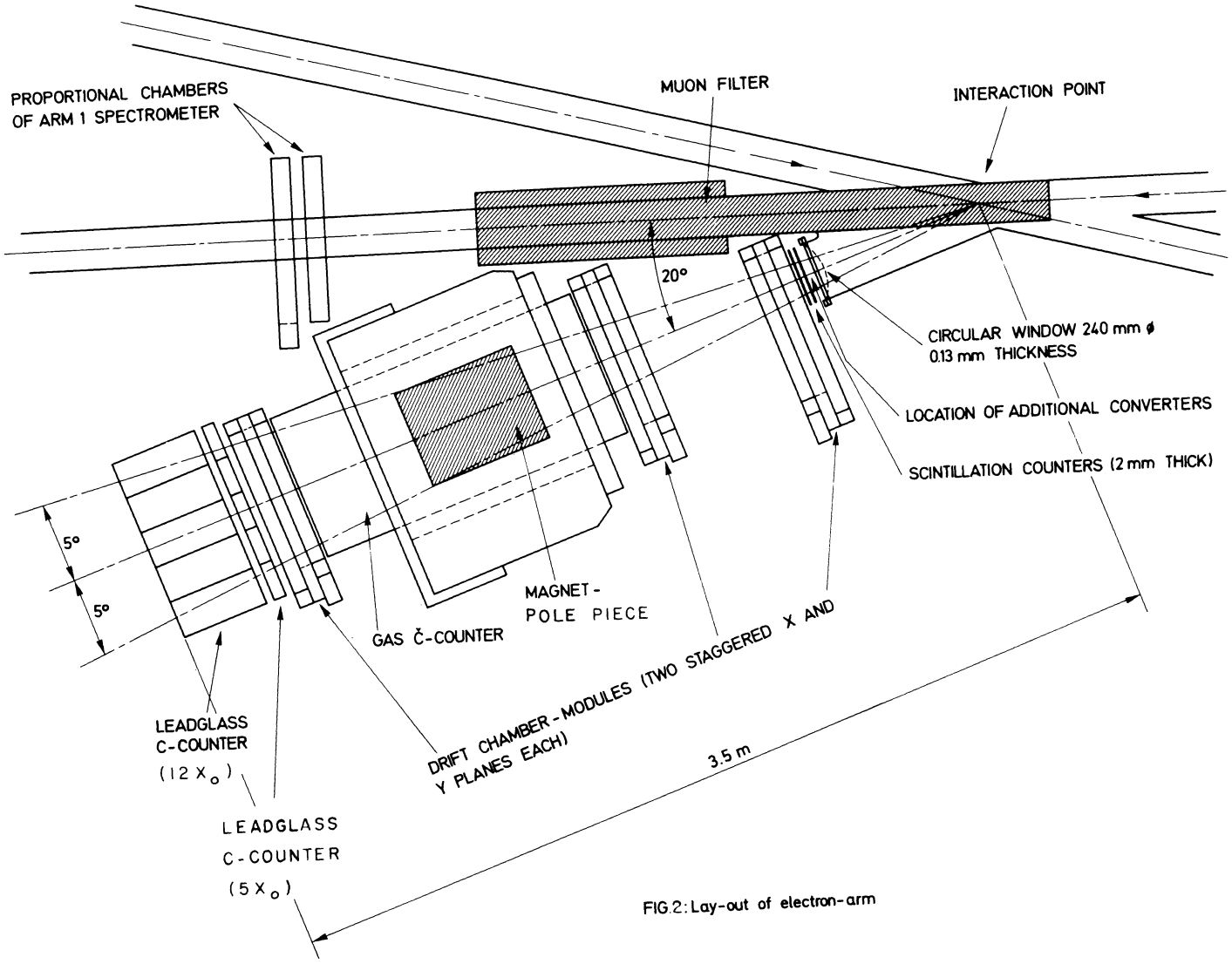

FIG.2: Lay-out of electron-arm

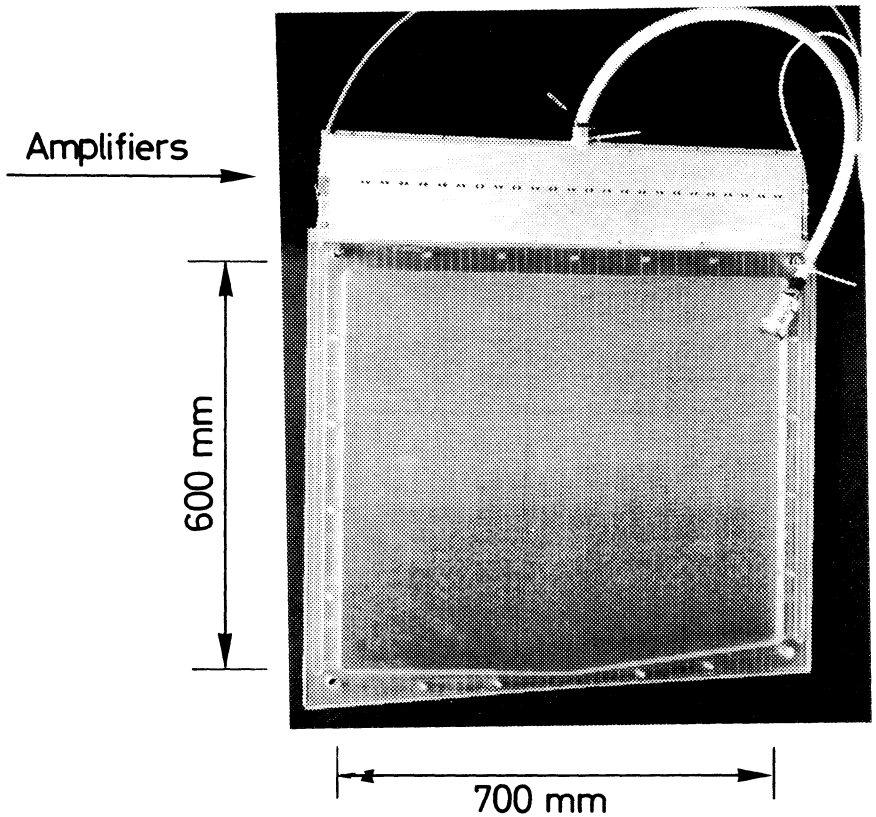

Driftchamber

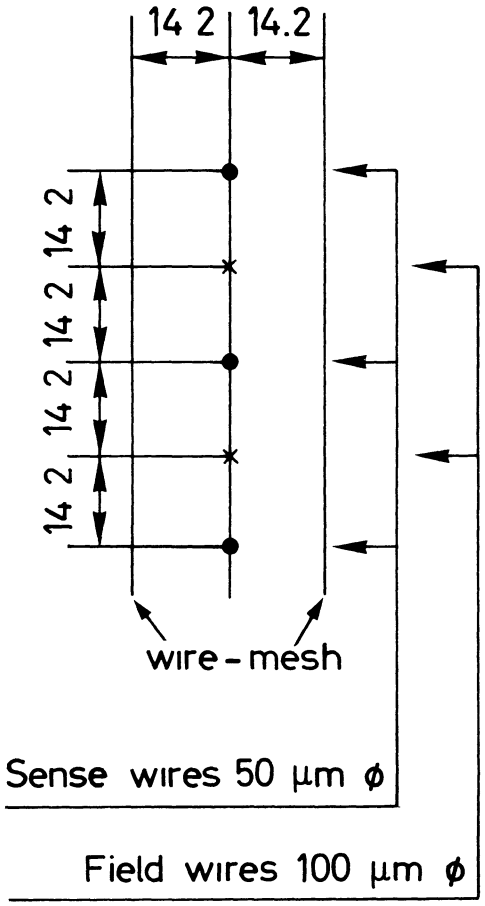

FIG. 3

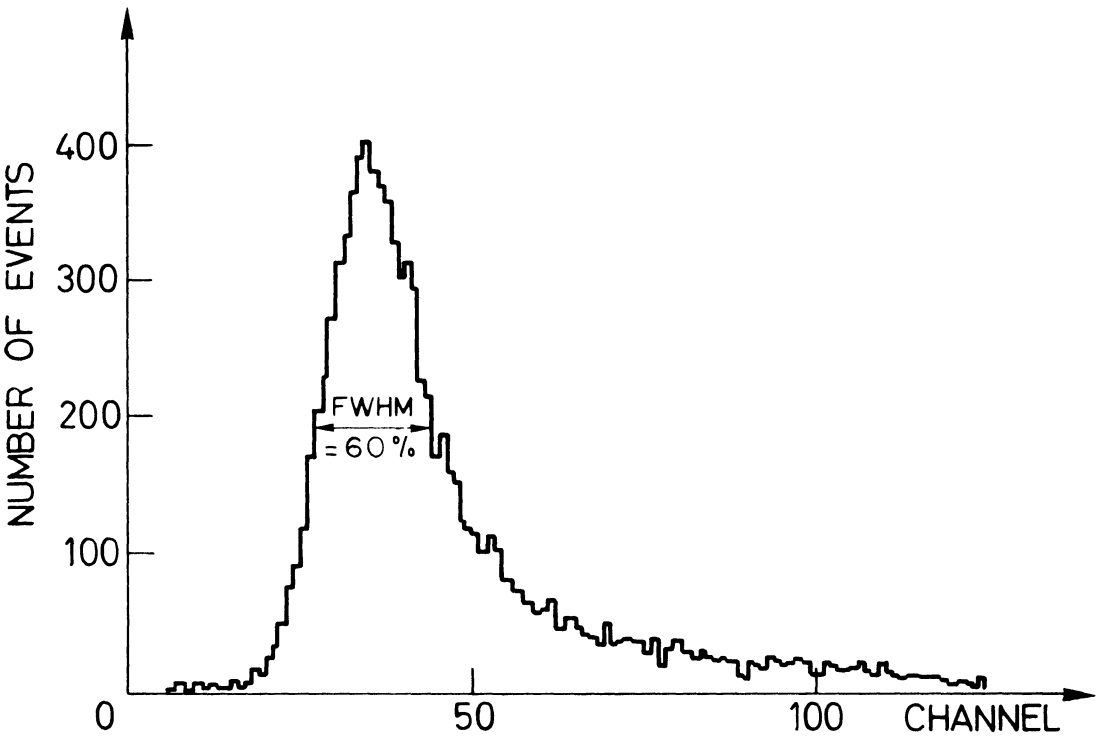

Pulse height distribution of 125 MeV pions

FIG. 4

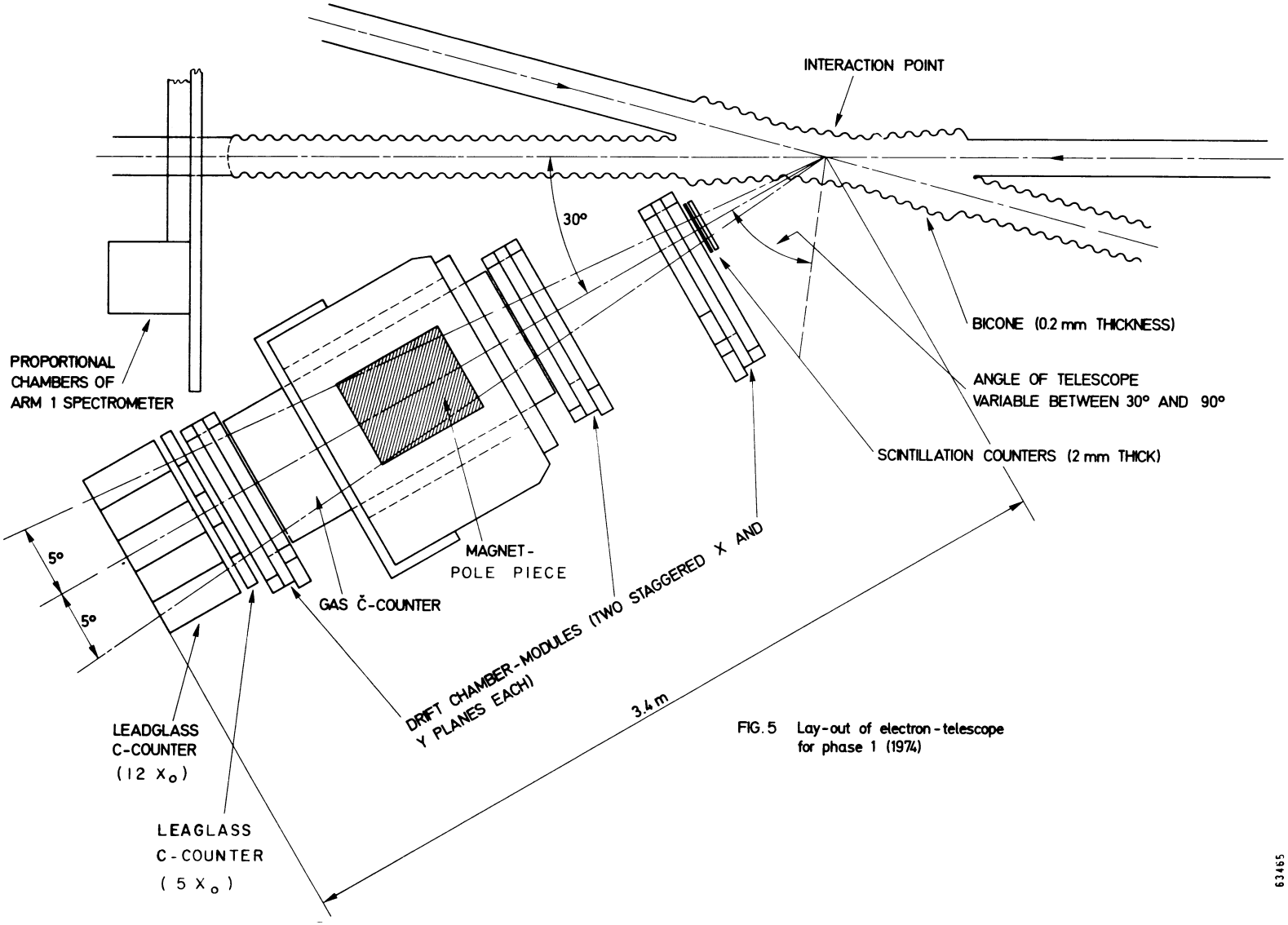

FIG. 5 Lay-out of electron-telescope for phase 1 (1974)

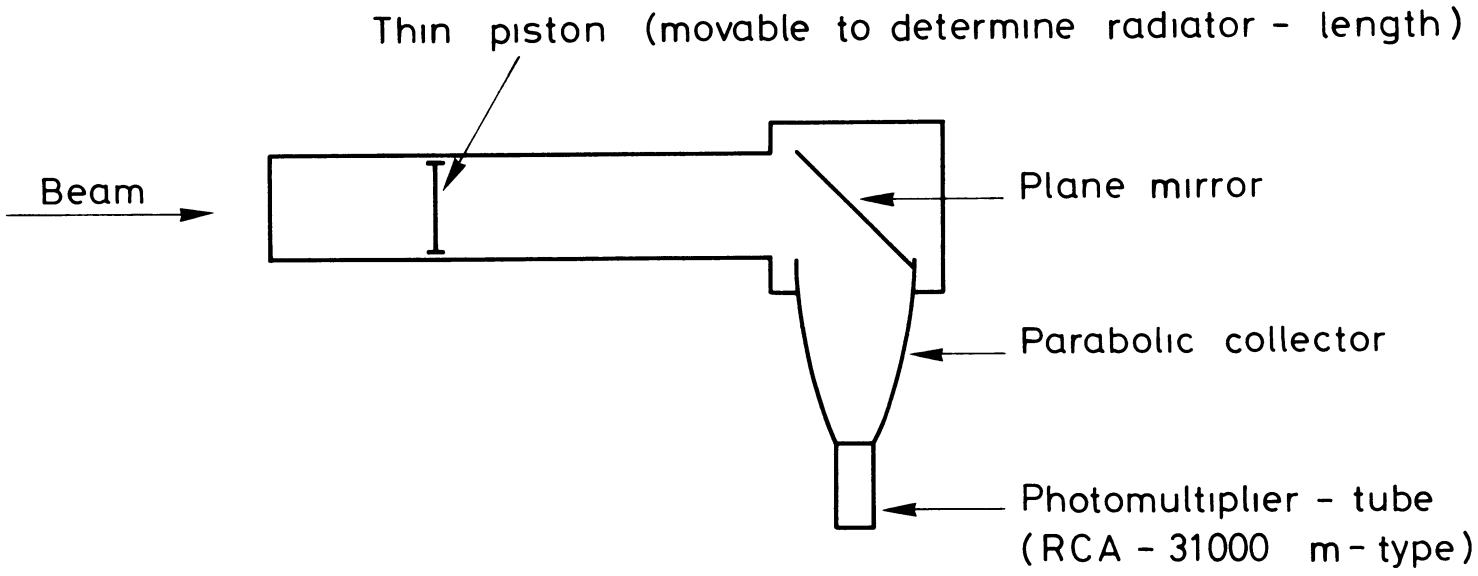
Thin piston (movable to determine radiator - length)
Beam
Plane mirror
Parabolic collector
Photomultiplier - tube
(RCA - 31000 m - type)

FIG 6

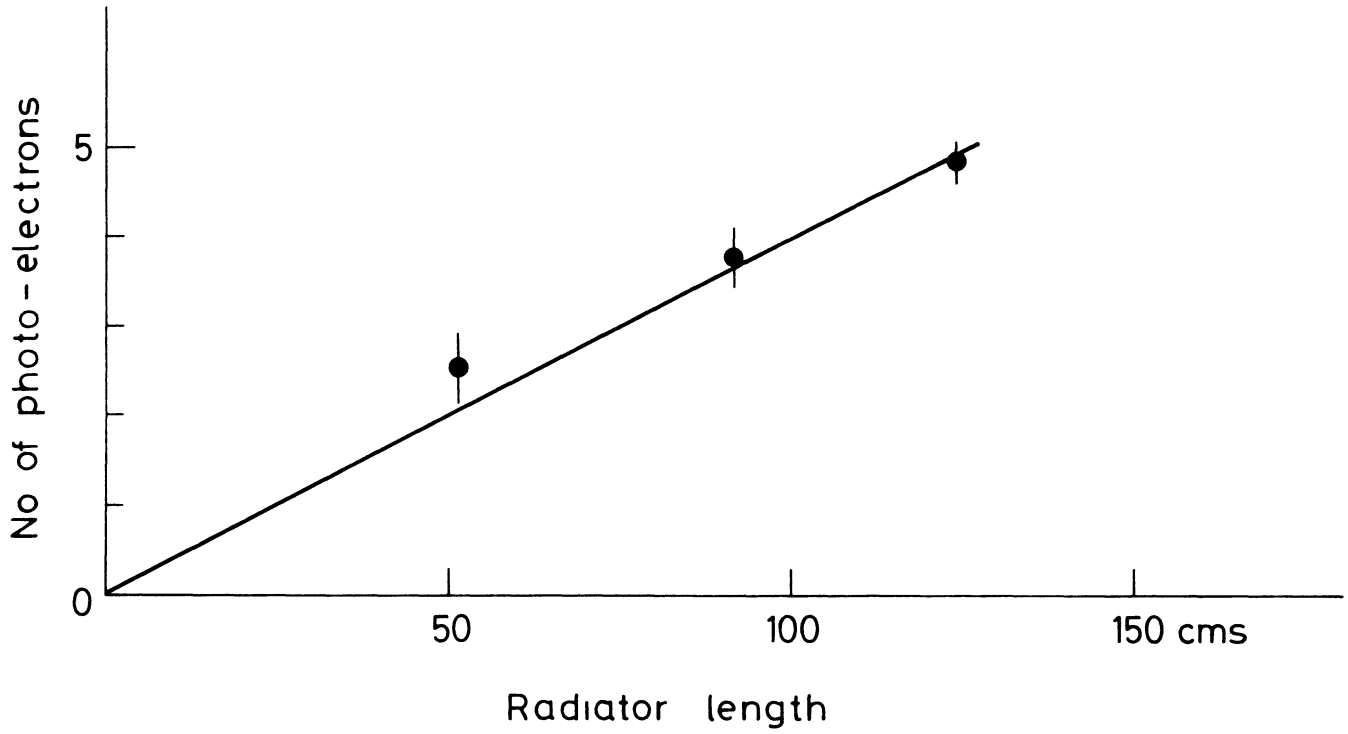

FIG. 7

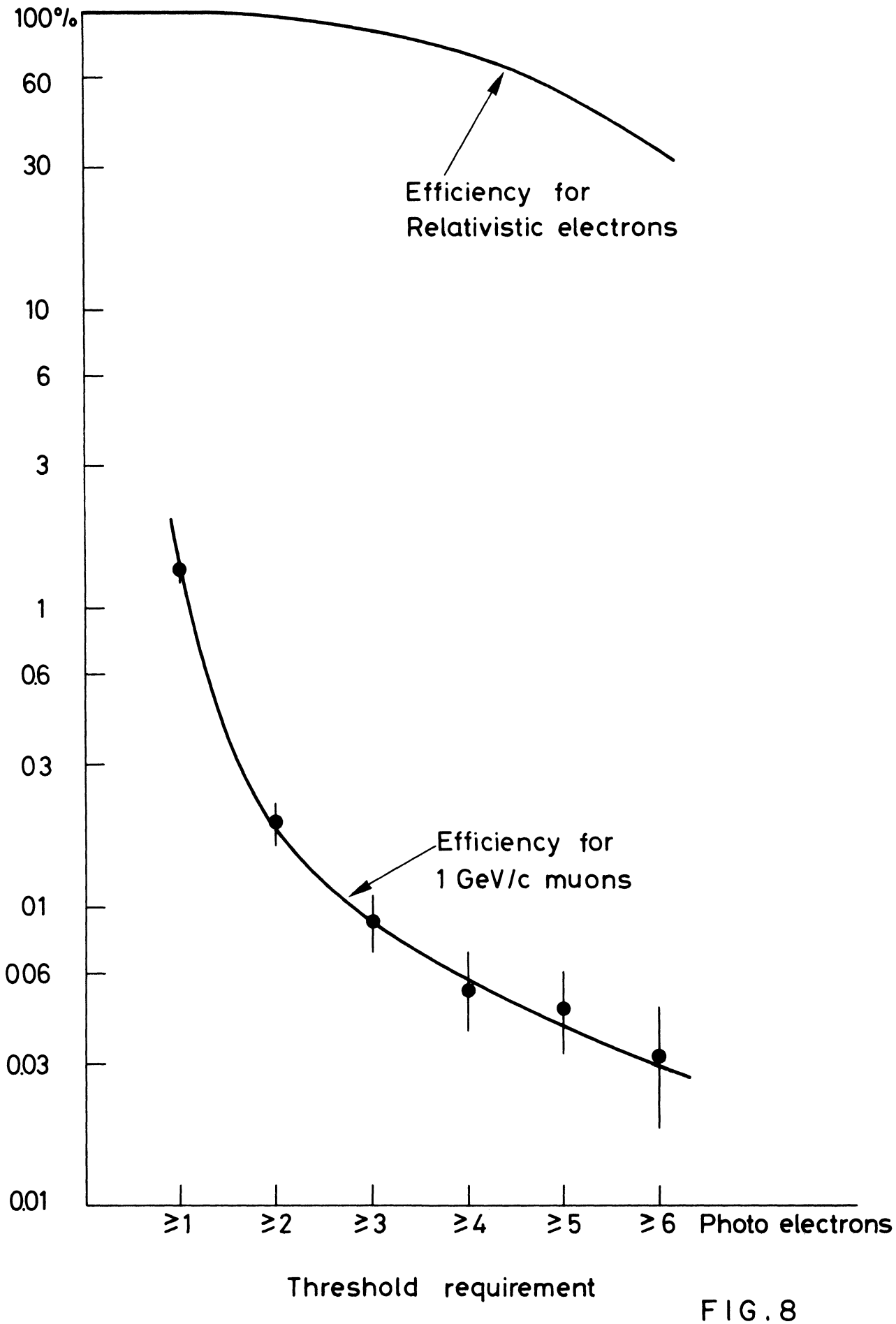
100%
60
30
10
6
3
1
0.6
0.3
0.1
0.06
0.03
0.01
Efficiency for
Relativistic electrons
Efficiency for
1 GeV/c muons
≥1
≥2
≥3
≥4
≥5
≥6
Photo electrons
Threshold requirement

FIG. 8

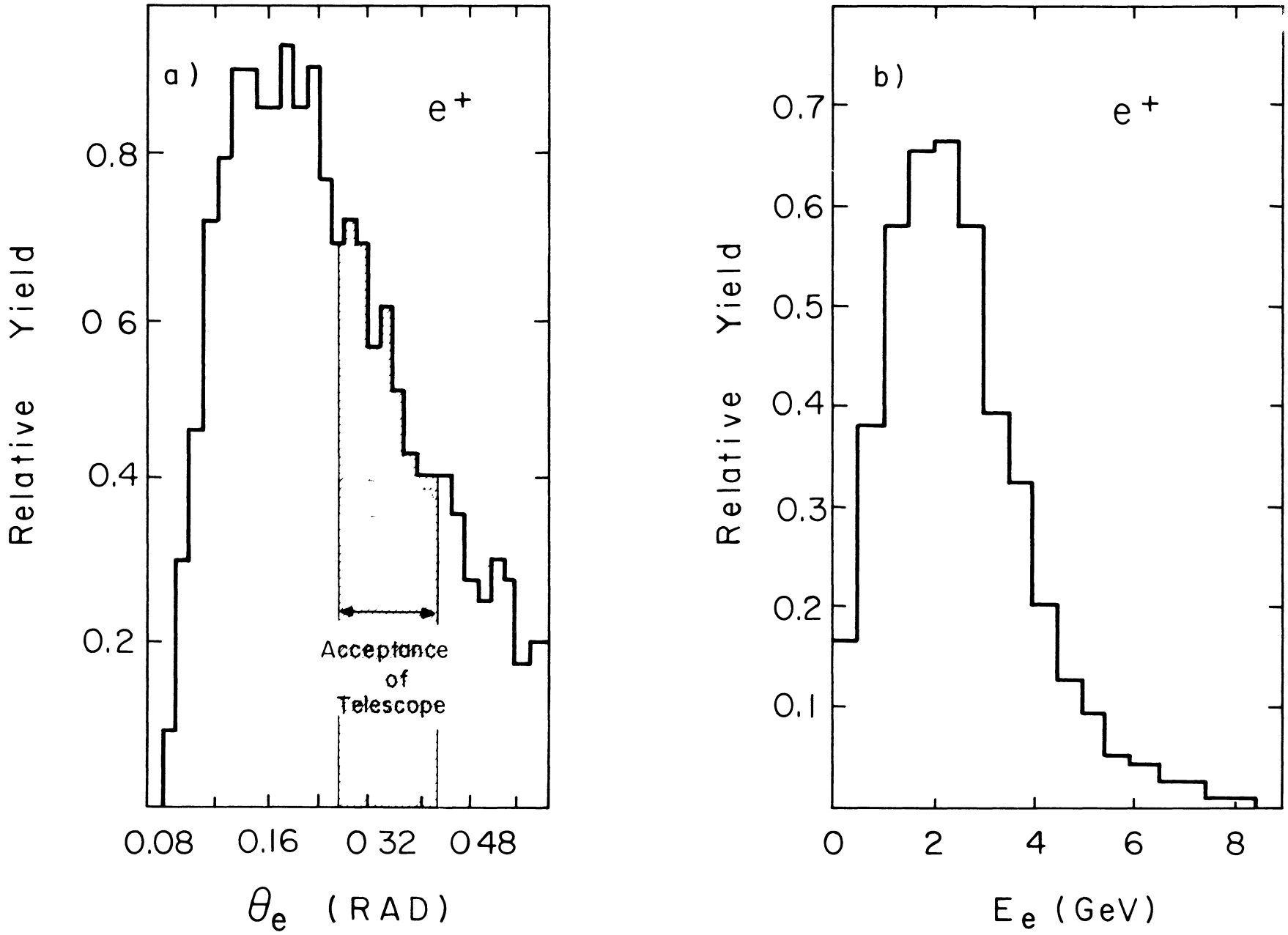
a)
e+
0.8
0.6
0.4
0.2
Relative Yield
Acceptance
of
Telescope
0.08
0.16
0 32
0 48
θe (RAD)
b)
e+
0.7
0.6
0.5
0.4
0.3
0.2
0.1
Relative Yield
0
2
4
6
8
Ee (GeV)

FIG. 9

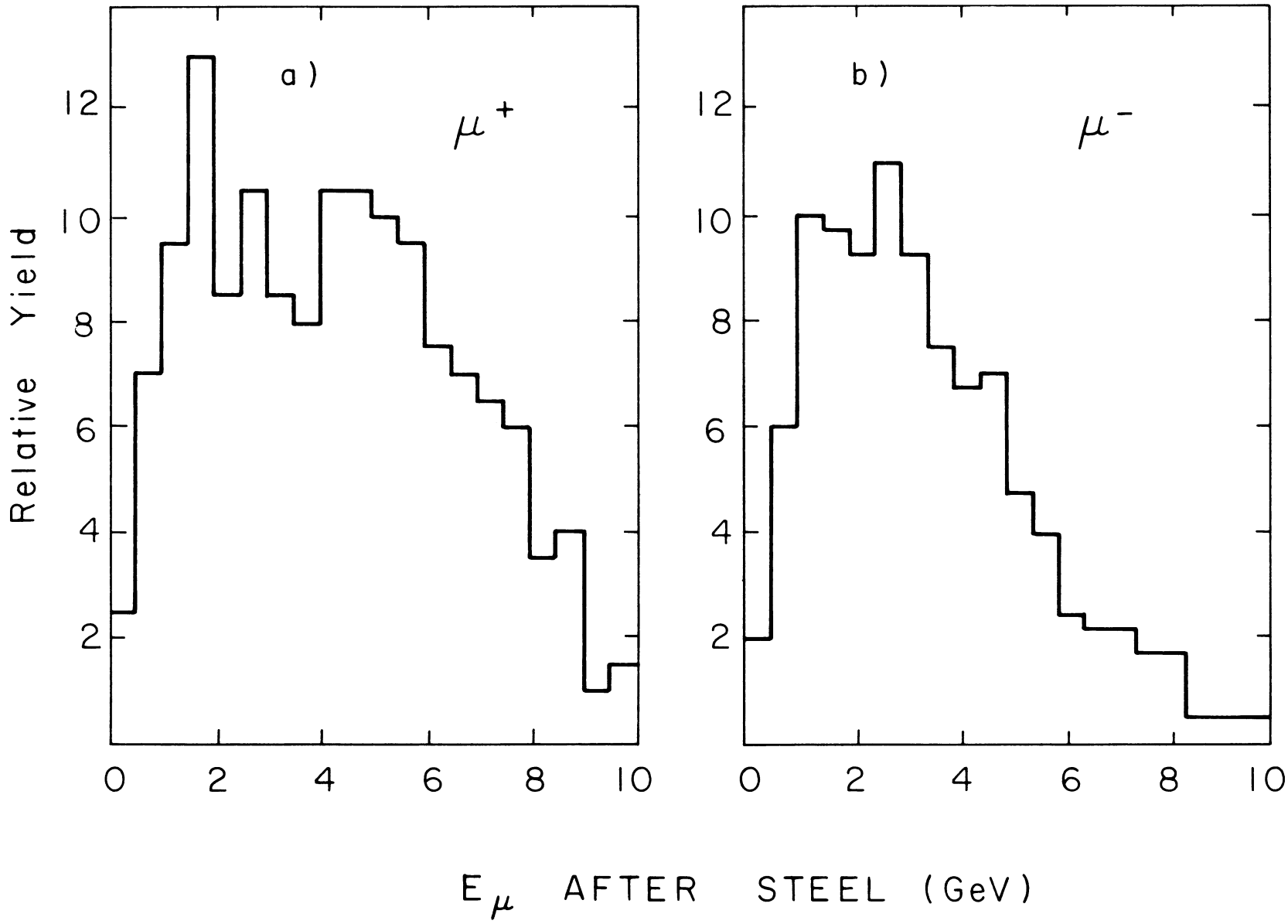

FIG. 10

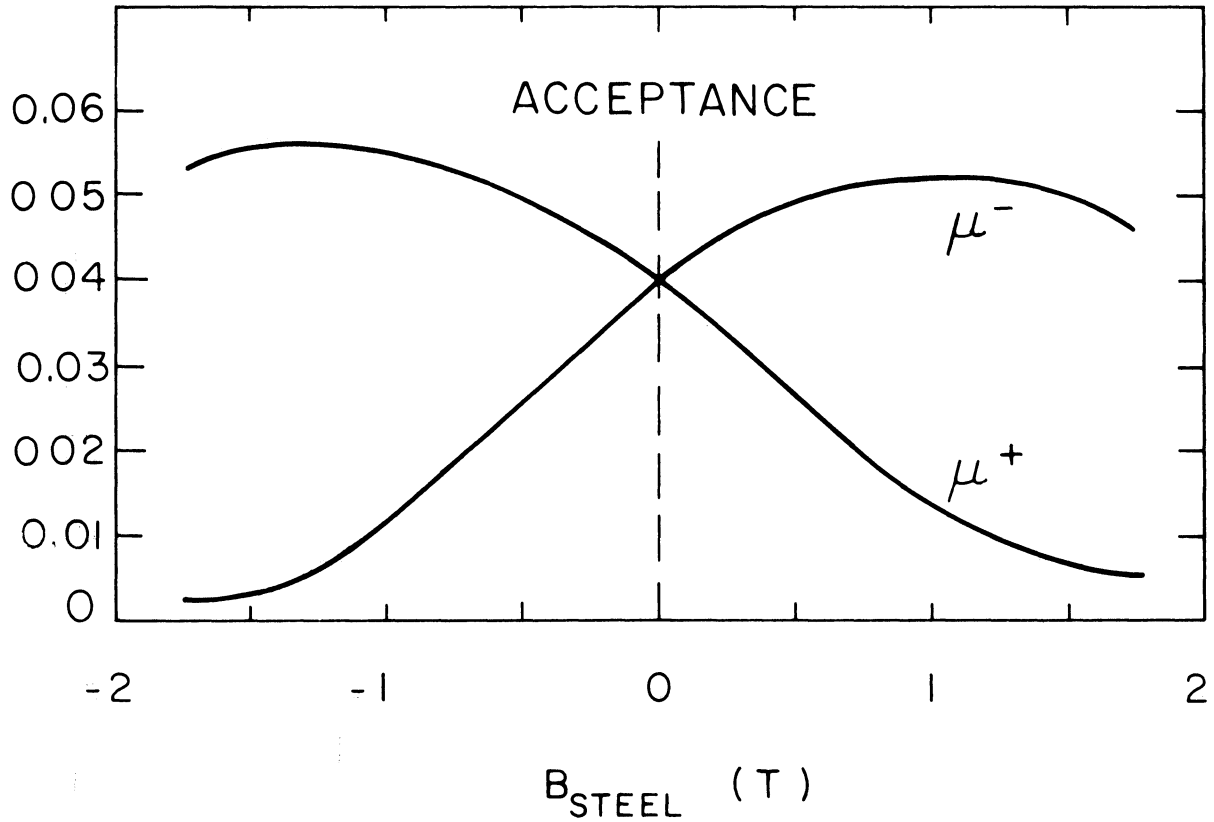

FIG. 11

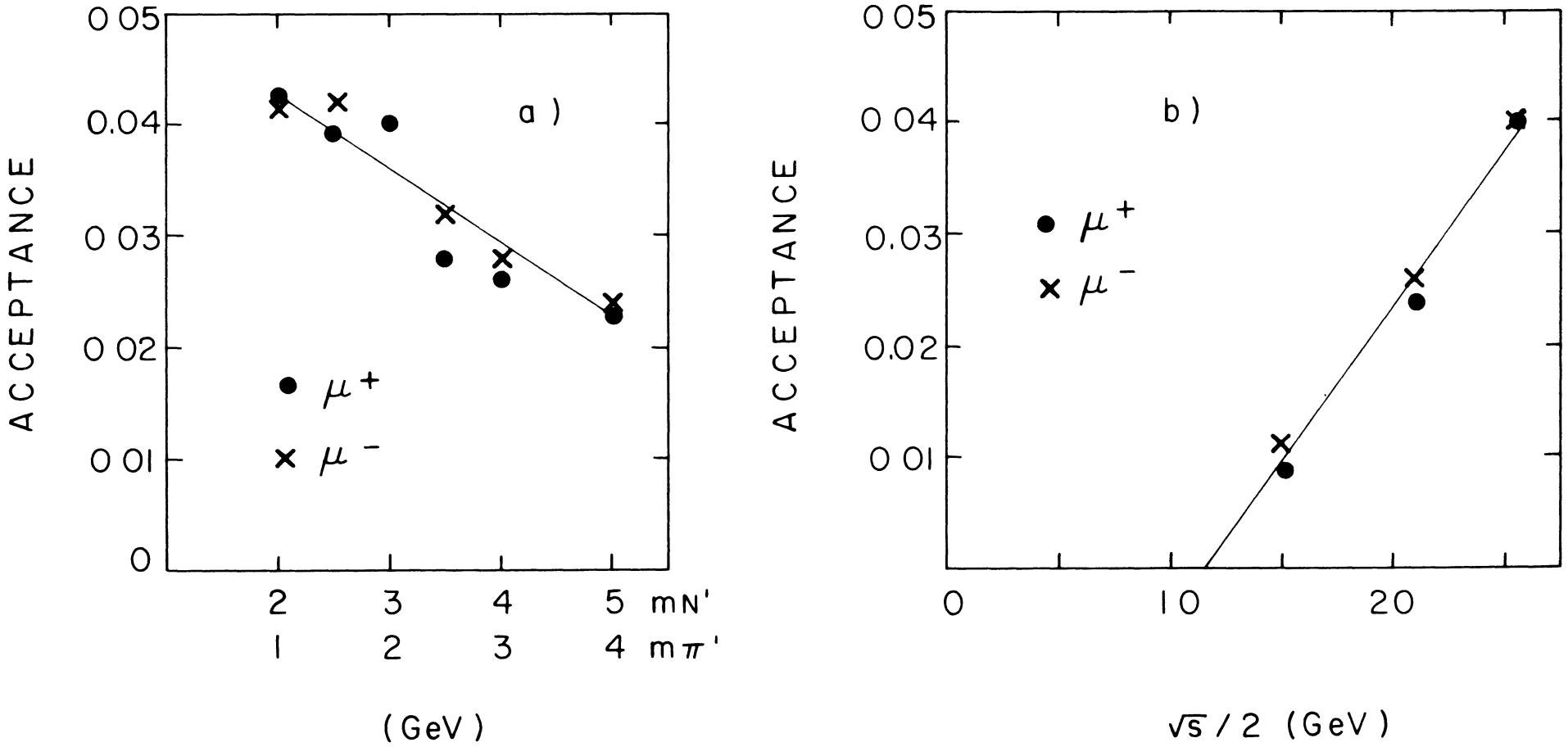
ACCEPTANCE
0 05
0.04
0 03
0 02
0 01
0
a)
μ^+
μ^-
2 3 4 5 mN'
1 2 3 4 mπ'
(GeV)
ACCEPTANCE
0 05
0 04
0.03
0.02
0 01
b)
μ^+
μ^-
0 10 20
√s / 2 (GeV)

FIG .12

APPENDIX

INTERNAL R-604 REPORT

M M. Block

THEORETICAL REMARKS ON A CHARMED SEARCH IN p-p COLLISIONS AT ISR ENERGIES

A1 INTRODUCTION

In this report, we assume that charmed particles are built up by adding a fourth quark p′ (with quantum numbers Q = 2/3, I = 0, S = 0, and charm C = +1) to the normal (p, n, λ) quark triplets of SU(3), in order to make an SU(4) symmetry. The types of baryons and bosons that can be found are illustrated in Table A1, the Charm Chart. We note that both strange and non-strange particles can be made, and that the baryon family can have charm quantum numbers C = 1, 2, or 3, whereas the bosons can only have C = 1 members We adopt the convention that positive charm is associated with particles, and negative charm for the antiparticles.

In this new scheme, the ordinary Cabbibo charged current (written in terms of quarks) for weak decays is generalized, in order to forbid strangeness-changing neutral currents to

$$J^+ = p\bar{n} \cos\theta_C + p\bar{\lambda} \sin\theta_C + p'\bar{\lambda} \cos\theta_C - p'\bar{n} \sin\theta_C + e^+\nu_e + \mu^+\nu_\mu \ , \qquad (1)$$

by adding the new p′ quark with the above coupling scheme. This current (1) then predicts that the p′ quark (the decay of physical charmed objects) is preferentially strangeness-changing, with the ratio of strangeness-changing transitions to non-strangeness-changing transitions being proportional to $\cot^2\theta_C$. Also shown in the Charm Chart are the favoured leptonic decay modes of charmed particles. As can be readily shown from the current (1), there is a selection rule for leptonic decays, $\Delta C = \Delta Q$, valid both for strangeness-changing non-strangeness-changing transitions, and this requires particles (C = positive, in our convention) to decay to positive leptons and antiparticles (C = negative) to decay into negative leptons

A2. PRODUCTION PROCESSES IN p-p COLLISIONS

Since charm is conserved in strong interactions, we basically have two mechanisms for charm production in p-p collisions, either pair production of the type $\pi'\bar{\pi}$, $N'\bar{N}'$, etc , or "associated charm" production, of the type $N'\bar{\pi}'$. We note in

passing that the production of $Y'\bar{K}'$ is forbidden, since although $\Delta C = 0$, $\Delta S \neq 0$ since the strangeness of $C = -1$ objects (the $\bar{K}'$'s) is -1. The pair production mechanism is similar to the pair production of $K\bar{K}$ and baryon-antibaryon production; it would be expected to exhibit a rather flat rapidity distribution, and would be important in a study of inclusive processes of large angles On the other hand, the mechanism of "associated charm" production, by analogy with ordinary YK processes, might be expected to be very important at x-values close to $|1|$, i e. for diffractive processes. In the following, we discuss the two mechanisms separately.

A Diffractive processes

The diffractive dissociation of a proton into $p \to \Lambda^0 K^+$ and $p \to N'^+ \bar{\pi}^{0\prime}$ can be pictorially visualized with the aid of quark diagrams, Fig. Ala and Alb, respectively

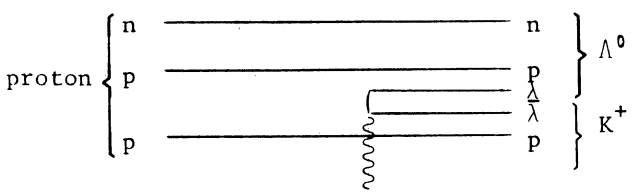

Fig Ala: Diffractive dissociation of $p \to \Lambda^0 K^+$

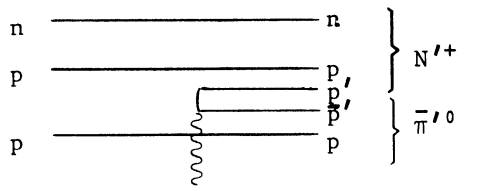

Fig Alb: Diffractive dissociation of $p \to N'^+ \bar{\pi}'^0$

We estimate the cross-section for the $N'\bar{\pi}'$ states as follows. Let $m_{N'}$ be the mass of N', $m_{\pi'}$ the $\bar{\pi}'$ mass, and $\mathcal{M}_{min} \equiv m_{N'} + m_{\pi'}$ is thus the mass threshold for the reaction $p + p \to p + \mathcal{M}$ The maximum mass for a diffractively-produced object in the above reaction, $\mathcal{M}_{max}$, can be estimated as a function of c.m.s. energy squared s, by the formula $\mathcal{M}^2 = s(1 - x)$, where we use $x_{min} \approx 0.9$, i.e. we estimate $\mathcal{M}^2_{max} = 0\ 1\ s$ The diffractive cross-section, for the mass region above the resonances, for the production of $\mathcal{M}^2$ in $d\mathcal{M}^2$, is known to go as

$$\frac{d\sigma}{d\mathcal{M}^2} = \frac{1\ mb}{\mathcal{M}^2} \tag{2}$$

Integrating Eq (2) between threshold ($\mathcal{M}^2_{min}$) and $\mathcal{M}^2_{max}$, we get

$$\sigma(\mathcal{M}^2_{min}, s) = \ln\left(\frac{0.1\ s}{\mathcal{M}^2_{min}}\right) mb \tag{3}$$

We now assume that we have an exact SU(4) symmetry that says, in the language of Figs. Ala and Alb, that the Pomeron is an equal admixture of $p\bar{p}$, $n\bar{n}$, $\lambda\bar{\lambda}$, and $p'\bar{p}'$ quarks. Hence, in this naive model, for masses $\mathcal{M}^2$ above $\mathcal{M}_{min}$, we assume that 1/4 of the cross-section goes into $N'\bar{\pi}'$, 1/4 into YK, and 1/2 into $N\pi$, with the states N', $\bar{\pi}'$, Y, K, N, π standing for ground or excited states with the appropriate quantum numbers. Hence we find in this model that the charmed cross-section σ_C is given by

$$\sigma_C(\mathcal{M}^2_{min}, s) = \frac{1}{4} \ln\left(\frac{0.1\ s}{\mathcal{M}^2_{min}}\right) \text{mb} \ . \tag{4}$$

In Table A2 we tabulate the diffractive cross-section for associated charm production as a function of the charmed particle masses, for an ISR experiment of 26 GeV on 26 GeV.

Table A2

Charm cross-section for 26 GeV on 26 GeV as a function of charmed masses

σ_C (mb)	$M_{N'}$ (GeV)	$M_{\pi'}$ (GeV)
0.85	2	1
0.60	3	2
0.43	4	3
0.30	5	4

At a first glance, these cross-sections seem to be very large. We can perhaps put these results into perspective by trying to compare them with experimental data on diffractive YK production. The quark diagrams Figs. Ala and Alb indicate that in our model, we expect an equal cross-section for YK and $N'\bar{\pi}'$, and that YK should also be 25% of the diffractive cross-section for masses above YK threshold. In Fig. A2 we show the inclusive Λ^0 spectra observed at FNAL in a bubble chamber experiment (as reported by M. Jacob at the 1972 Batavia Conference), and we see a charge concentration of events for $|x|$ near 1. Subtracting a smooth background, these data yield a cross-section for (presumably) diffractive Λ^0's of $\sim$ 1/3 of total Λ^0 production, i.e. a diffractive cross-section of about 0.6 mb in each hemisphere. For 200 GeV, applying Eq. (4) (used to predict equal YK and $N'\pi'$ yields) to YK production, we calculate 0.8 mb. This prediction, considering the fact that total YK production includes $\Sigma^{\pm}$ as well (unobserved in the experiment), is in good agreement with the experimental lower limit of 0.6 mb.

It is appropriate at this point to comment on the choice of masses used for Table A2. According to Gaillard[1], the mass of the p′ quark should not be much greater than that of the other quarks; or weak interactions, in calculations of second-order diagrams, would be in difficulty. Hence, we adopt the simplifying procedure that the π' (containing two quarks) weighs about 1 GeV less than the N′ (which has three quarks), and that they cannot have physical masses much greater than several GeV

In summary, we expect a diffractive cross-section of $\sim$ 1/2 mb. Furthermore, we expect the pion multiplicity of non-charmed diffractive events to correspond to a rather low pion multiplicity, a result of some importance for estimating background to leptonic decay modes of N′ and $\bar{\pi}'$. As a figure of merit, we estimate that $\sigma_C/\sigma_\pi \approx 3 \times 10^{-2}$, where σ_π is the pion cross-section.

B Inclusive production

FNAL data on inclusive muon production[2,3,4] as well as the FNAL[4] and the ISR[5] data on electron production yield the interesting conclusions that the rates for inclusive production of e^+, e^-, μ^+, and μ^- are all equal (within errors) and that this rate, expressed as a fraction of observed leptons to observed pions, is $n_\ell/n_\pi \approx 10^{-4}$, independent of production variables If we attempt to explain this result by leptonic decays of charmed objects, and if we assume the same efficiency for detecting the leptonic decay particles as for pions, it implies that if σ_π is the total changed pion cross-section; and if we call BR the branching ratio of charmed particles into leptons (we assume that the branching ratio to muons equals that for electrons), and define σ_C to be the cross-section for inclusive production of charmed particles, then

$$\frac{\sigma_C \cdot BR}{2\sigma_\pi} = 10^{-4} \ . \tag{5}$$

Thus, from Eq. (5), and using $\sigma_\pi \approx 250$ mb, we get

$$\sigma_C \approx \frac{50\ \mu b}{BR} \tag{6}$$

---

1) M. Gaillard, FNAL Conference, 74/43-THY.

2) J. Cronin et al., 17th Int. Conf. on High-Energy Physics, London, 1974.

3) C. Rubbia, private communication

4) L. Lederman et al , 17th Int. Conf on High-Energy Physics, London, 1974.

5) A. Di Lella et al , 17th Int. Conf. on High-Energy Physics, London, 1974.

The total cross-section for inclusive production of charm, as well as the ratio of σ_C/σ_π, useful for background estimates, is tabulated in Table A3, as a function of BR → leptons.

Table A3

Inclusive charm cross-section, as a function of BR → leptons

σ_C(mb)	BR → leptons	σ_C/σ_π
0.05	1	2×10^{-4}
0.50	0.1	2×10^{-3}
5 00	0.01	2×10^{-2}

For a branching ratio of 0.10, we again get a cross-section of 0.5 mb, with a ratio of $\sigma_C/\sigma_\pi \approx 2 \times 10^{-3}$. We recall that for the diffractive process, the ratio was 3×10^{-2}, a significantly better signal-to-noise situation for the detection of leptonic modes

C. Decay modes of charmed particles

The current in Eq. (1) completely determines the leptonic decay rates for the three-body decays

$$N' \to Y\ell^+\nu_\ell \tag{7a}$$

and

$$\bar{\pi}' \to K\ell^-\bar{\nu}_\ell \ . \tag{7b}$$

As previously emphasized, these strangeness-changing decays (by a factor of $\sim$ 15) dominate over their companion modes

$$N' \to N\ell^+\nu_\ell \tag{8a}$$

and

$$\bar{\pi}' \to \pi\ell^-\bar{\nu}_\ell \ . \tag{8b}$$

The partial decay rate for expression (7a) can readily be shown to be given by*)

$$\Gamma = \frac{\cos^2\theta_C}{\tau_\mu}\left(\frac{m_{N'}}{m_\mu}\right)^5 \left\{(1+x^2)\left[\left(\frac{1-8\alpha^2+\alpha^4}{2}\right) - 12\alpha^4 \ln\alpha\right] + \right.$$

$$\left. + (x^2-1)\alpha\left[(1+10\alpha^2+\alpha^4)(1-\alpha^2) + 3\alpha^2(1+\alpha^2)\ln\alpha\right]\right\} \text{sec}^{-1} \ , \tag{9}$$

where σ_C is the Cabbibo angle, m_μ the muon mass, τ_μ the muon lifetime in seconds, $m_{N'}$ the mass of the charmed baryon, m_Y the hyperon mass, the parameters $\alpha \equiv m_Y/m_{N'}$,

*) In (9) the lepton mass has been set equal to zero.

and x the amount of axial vector strength present in the interaction V - xA assumed in calculating Eq (9) To apply formula (8) to formula (8a), we simply replace $\cos^2 \theta_C$ by $\sin^2 \theta_C$ and redefine $\alpha = m_N/m_{N'}$. To get an estimate of the partial lifetime $1/\Gamma$ for expression (7a), where Y is the Λ^0 and $m_{N'} = 3$ GeV, for $x = 1$ (V - A theory), we get 3×10^{-13} sec, indicating that the actual lifetime (due to summing over the decay ratio to all channels) is probably $\lesssim 10^{-13}$ sec. Because of their high masses, we expect that the channel particles decay in a very short time, undecaying predominantly strangeness-changing transitions, mainly into three or more bodies. The last remark follows because two-body phase space saturates with energy release, whereas from formula (9), for small α, $\Gamma_{3\text{-body}}$ goes as $(m_{N'})^5$. Furthermore, the rates are the same for both muons and electrons, since the muon rest mass is negligible in the problem

In order to do an experiment to detect the leptonic decay modes of charmed particles, it is critical to know the leptonic branching ratio (BR → leptons). This is a rather delicate point, since the theoretical guides are tremendously complicated by strong interaction physics, effects that are at best difficult to estimate reliably For example, the transitions (using the quark picture):

$$p' \to \lambda \ell^+ \nu \qquad (10a)$$

and

$$p' \to \lambda p \bar{n} \quad , \qquad (10b)$$

where expression (10a) describes charmed leptonic decay and (10b) non-leptonic decays, have rates proportional to $\cos^2 \theta_C$ and $\cos^4 \theta_C$, respectively, i.e. their ratio is ~ 1. Since there are equal leptonic transitions to ℓ being either μ or e, we conclude that the charmed branching ratio to leptons is 2/3. On the other hand, the same model used to describe strange particle decays, e.g. kaon decay, gives

$$p\bar{\lambda} \to \ell^+ \nu \qquad (11a)$$

and

$$p\bar{\lambda} \to p\bar{n} \quad , \qquad (11b)$$

where process (11a) describes lepton decay and (11b) mesonic channels, with rates proportional to $\sin^2 \theta_C$ and $\sin^2 \theta_C \cos^2 \theta_C$, respectively, thus, also giving a ratio ~ 1. However, although process (11a) describes the leptonic decay very well, the influences of strong interactions apparently causes (11b) to be enhanced to the order of unity, i.e augmented by a factor of $\sim 1/\sin^2 \theta_C$, an argument which was pointed out by Gaillard[1]. Thus, the branching ratio into leptons becomes $\sim 2 \sin^2 \theta_C$, i.e $\sim 10\%$. Hence values of BR → leptons between ~ 0.1 and 0.7 seem a reasonable range for the design of experiments.

Table A1: Charm Chart

Particle family name	C	S	B	I	I_z	Q	Quark composition	Favoured types of leptonic decay modes
π'	+1	0	0	½	+½	+1	$p'\bar{n}$	$\pi'^{+} \to \bar{K}^0\ell^+\nu$, $K^-\pi^+\ell^+\nu$, $K^-\pi^0\ell^+\nu$
					−½	0	$p'\bar{p}$	$\pi'^{0} \to K^-\ell^+\nu$, $\bar{K}^0\pi^-\ell^+\nu$
K'	+1	+1	0	0	0	+1	$p'\bar{\lambda}$	$K'^{+} \to \pi^+\pi^-\ell^+\nu$
N'	+1	0	+1	1	+1	+2	$p'pp$	$N_1'^{++} \to \Sigma^+\ell^+\nu$, $\Sigma^0(\Lambda^0)\pi^+\ell^+\nu$
					0	+1	$p'pn$	$N_1'^{+} \to \Sigma^0(\Lambda^0\pi^0)\ell^+\nu$, $\Sigma^{\mp}\pi^{\pm}\ell^+\nu$
					−1	0	$p'nn$	$N_1'^{0} \to \Sigma^-\ell^+\nu$, $\Sigma^0(\Lambda^0)\pi^-\ell^+\nu$
				0	0	+1	$p'pn$	$N_0^{+} \to \Sigma^0\pi^0(\Lambda^0)\ell^+\nu$, $\Sigma^{\mp}\pi^{\pm}\ell^+\nu$
Λ'	+1	−1	+1	½	+½	1	$p'p\lambda$	$\Lambda'^{+} \to \Xi^0\ell^+\nu$, $\Xi^-\pi^+\ell^+\nu$
					−½	0	$p'n\lambda$	$\Lambda'^{0} \to \Xi^-\ell^+\nu$, $\Xi^0\pi^-\ell^+\nu$
Ξ'	+1	−2	+1	0	0	0	$p'\lambda\lambda$	$\Xi'^{0} \to \Omega^-\ell^+\nu$

Rules: 1) $\Delta C = \Delta Q$ for <u>all</u> leptonic decays

2) $\Delta S = \Delta Q$ for strangeness-changing leptonic decays, $\Delta I = 0$

Possible production mechanism in strong interactions ($\Delta S = 0$, $\Delta Q = 0$, $\Delta B = 0$, $\Delta C = 0$)

1) Pair production $\pi'\bar{\pi}'$, $K'\bar{K}'$, $N'\bar{N}'$, $\Lambda'\bar{\Lambda}'$, $\Xi'\bar{\Xi}'$,

2) "Associated Charm" production proton $\to (N'\bar{\pi}')^+$

neutron $\to (N'\bar{\pi}')^0$

Note: we <u>cannot</u> have proton $\not\to (\Lambda'\bar{K}')^+$ or neutron $\not\to (\Lambda'\bar{K}')^0$ } since $\Delta S \neq 0$ although $\Delta C = 0$,

but we <u>can</u> have proton $\to (\Lambda'\bar{K}'KK)^+$

and proton $\to (\Xi'\bar{K}'KKK)^+$, etc.,

3) We <u>expect diffractive production</u> of $p \to N'^{++}\overline{\pi'^{+}}$ and $N'^{0}\overline{\pi'^{0}}$, in analogy to $YK \left\{\begin{matrix}\Sigma^+K^0\\ \Sigma^0(\Lambda^0)K^+\end{matrix}\right\}$.

Table A1 (cont.): Charm Chart

Particle Family Name	C	S	B	I	I_z	Q	Quark composition	Favoured types of leptonic decay modes
N''	+2	0	1	$\frac{1}{2}$	$+\frac{1}{2}$	+2	$p'p'p$	$N''^{++} \rightarrow \Lambda'^{+}\pi^{+}(\pi^{0})$ / $\Lambda'^{0}\pi^{+}\pi^{+}$
					$-\frac{1}{2}$	+1	$p'p'n$	$N''^{+} \rightarrow \Lambda'^{+}\pi^{0}(\pi^{0})$ / $\rightarrow \Lambda'^{0}\pi^{+}$
								and, in a second weak decay, the Λ''s decay into Ξ's and $\ell^{+}\nu$
Λ''	+2	-1	1	0	0	+1	$p'p'\lambda$	$\Lambda''^{+} \rightarrow \Xi'^{0}\pi^{+}$ and, in a second decay, $\Xi'^{0} \rightarrow \Omega^{-}\ell^{+}\nu$
N'''	+3	0	1	0	0	+2	$p'p'p'$	$N'''^{++} \rightarrow \Lambda''^{+} + \pi^{+}$, and, in next decay $\Lambda''^{+} \rightarrow \Xi'^{0}\pi^{+}$, and in next decay $\Xi'^{0} \rightarrow \Omega^{-}\ell^{+}\nu$

1) Strong interaction production mechanisms:

a) Pair production: $N''\overline{N''}$, $\Lambda''\overline{\Lambda''}$, $N'''\overline{N'''}$

b) "associated charm" production proton $\rightarrow (N''\bar{\pi}'\bar{\pi}')^{+}$, $(\Lambda''\bar{K}'\bar{K}'KKK)^{+}$, $(N'''\bar{\pi}'\bar{\pi}'\bar{\pi}')^{+} + (N'''\bar{K}'\bar{\pi}'\bar{\pi}'K)^{+}$, etc

Note: No C = +2 or +3 (multiple charm) mesons are possible

Notation: Quark
- p' : I = 0, Q = $\frac{2}{3}$
- p : I = $\frac{1}{2}$, Q = $\frac{2}{3}$
- n : I = $\frac{1}{2}$, Q = $-\frac{1}{3}$
- λ : I = 0, Q = $-\frac{1}{3}$

I = isospin — I_z = z-component of I

Q = charge — B = baryon number

S = strangeness — C = charm (0, ±1, ±2)

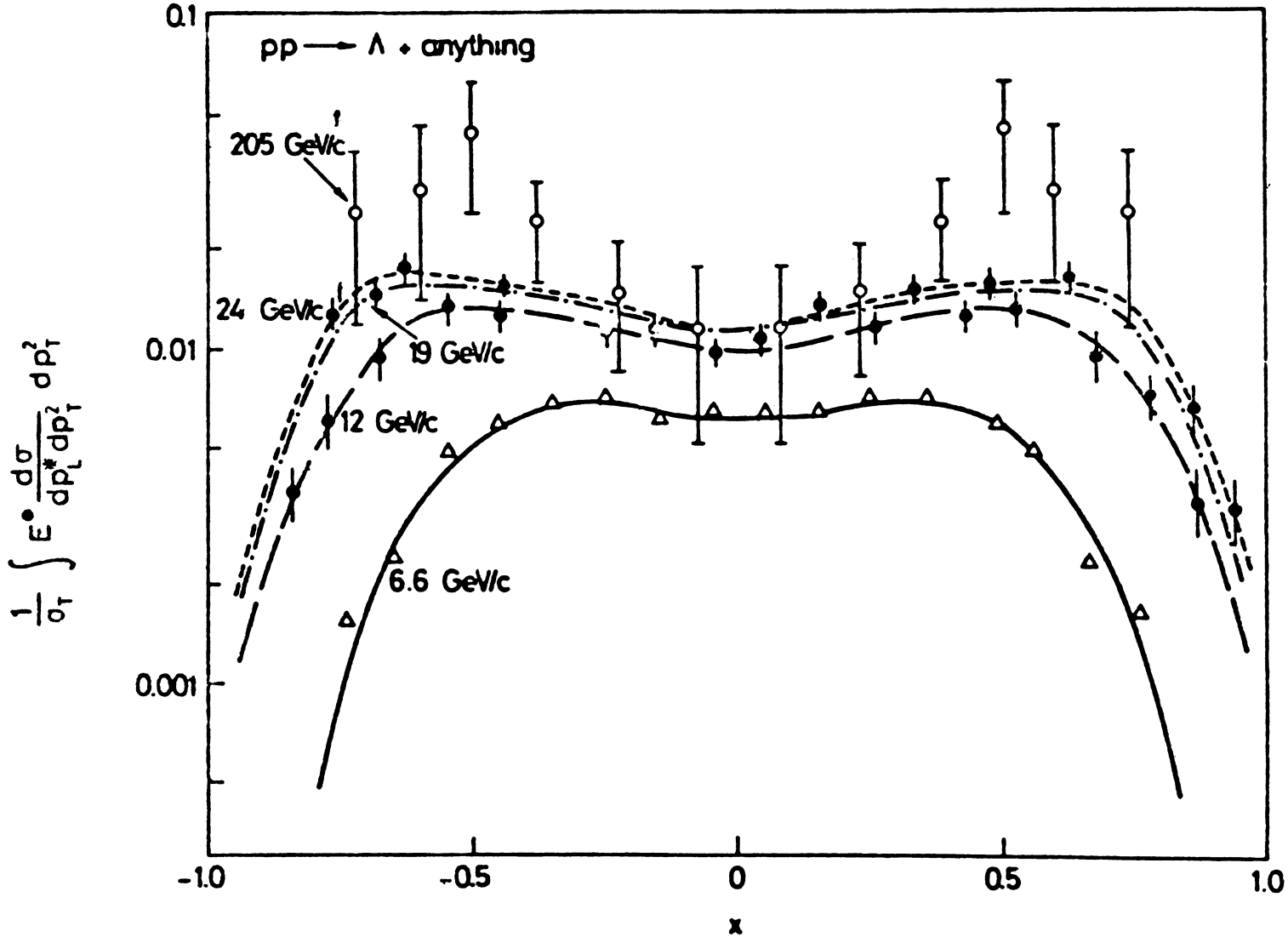
pp → Λ + anything
205 GeV/c
24 GeV/c
19 GeV/c
12 GeV/c
6.6 GeV/c
0.1
0.01
0.001
-1.0
-0.5
0
0.5
1.0
x
$\frac{1}{\sigma_T}\int E^* \frac{d\sigma}{dp_L^* dp_T^2} dp_T^2$

Fig A2